RESEARCH ARTICLE

Secretome-based proteomics reveals sulindac-modulated proteins released from colon cancer cells

Hong Ji, David W. Greening, Eugene A. Kapp, Robert L. Moritz and Richard J. Simpson

Joint Proteomics Laboratory, Ludwig Institute for Cancer Research and the Walter and Eliza Hall Institute of Medical Research, Parkville, Victoria, Australia

Although experiments in rodents and human population-based studies have demonstrated the efficacy of nonsteroidal anti-inflammatory drugs (NSAIDs) such as sulindac in colorectal cancer (CRC) prevention, a detailed knowledge of the underlying mechanism of action of this drug is limited. To better understand the chemopreventitive effects of sulindac, especially early sulindac-induced apoptotic events, we used the CRC cell line LIM1215 as an experimental model, focusing on proteins secreted into the LIM1215 culture medium – *i.e.*, the secretome. This subproteome comprises both soluble-secreted proteins and exosomes (30–100 nm diameter membrane vesicles released by several cell types). Selected secretome proteins whose expression levels were dysregulated by 1 mM sulindac treatment over 16 h were analyzed using 2-D DIGE, cytokine array, Western blotting, and MS. Overall, 150 secreted proteins were identified, many of which are implicated in molecular and cellular functions such as cell proliferation, differentiation, adhesion, invasion, angiogenesis, metastasis, and apoptosis. Our secretome-based proteomic studies have identified several secreted modulators of sulindac-induced apoptosis action (*e.g.*, Mac-2 binding protein, Alix, 14-3-3 isoforms, profilin-1, calumenin/Cab45 precursors, and the angiogenic/tumor growth factors interleukin 8 (IL-8) and growth related oncogene (GRO-α)) that are likely to improve our understanding of the chemopreventitive action of this NSAID in CRC.

1 Introduction

Colorectal cancer (CRC) is the third commonest malignancy in western populations [1], responsible for approximately 150 000 new patients and approximately 50 000 deaths *per* year in the United States alone (SEER Cancer Statistics Review 1975–2004, National Cancer Institute 2007: http://seer.cancer.gov/csr/1975_2004/results_single/sect_01_table.01.pdf). Despite these statistics, CRC is treatable when the disease is localized and detected at an early stage. Most CRCs develop from precursor adenomas, which can be identified by colonoscopic and/or sigmoidoscopic screening and removed by polypectomy [2]. While these treatments significantly reduce mortality from CRC, there is now mounting evidence from randomized, controlled trials that they can be augmented by the use of chemopreventitive agents such as nonsteroidal anti-inflammatory drugs (NSAIDs) [3]. NSAIDs have a demonstrated efficacy in reducing recurrent adenomas and malignant transformation of precursor adenomas in patients with the unusual hereditary condition familial adenomatous polyposis (FAP) [4]. Modest chemopreventitive effects of NSAIDs have also been reported for sporadic colorectal adenomas using population-based randomized trials for aspirin [5, 6] and celecoxib [7].

Correspondence: Professor Richard J. Simpson, Ludwig Institute for Cancer Research, PO Box 2008, Royal Melbourne Hospital, Royal Parade, Parkville, Victoria 3050, Australia
E-mail: richard.simpson@ludwig.edu.au
Fax: +61-03-9341-3104

Abbreviations: ALG-2, apoptosis-linked gene 2; **CRC,** colorectal cancer; **EM,** electron microscopy; **GRO,** growth related oncogene; **IL-8,** interleukin 8; **MTT,** 3-(4,5-dimethylthiazol-2-yl)-2,5-diphenyltetrazolium bromide; **PPAR,** peroxisome proliferator-activated receptor; **SFM,** serum-free media

The NSAID sulindac and selective cycloxygenase (COX)-2 inhibitors all prevent tumor formation in a variety of rodent models [8–13]. (Physiologically, sulindac is metabolized in the colon to sulindac sulfide and sulindac sulfone; the sulfide derivative inhibits colon carcinogenesis by inhibiting COX-1 and COX-2 enzyme activity [14].) Polymorphisms in genes encoding NSAID-metabolizing enzymes [15] (for a review, see [16]) as well as ornithine carboxylase [17] modulate this chemopreventitive effect. Interindividual genetic differences in the absorption, metabolism, and excretion of NSAIDs may, in part, explain the pharmacokinetic variability in the response to NSAIDs, including sulindac, as well as specific COX-2 inhibitors [16, 18]. (Because of potential cardiovascular events, the COX-2-specific inhibitors celecoxib [7] and rofecoxib [19] cannot be routinely recommended for this indication.)

While evidence supporting the ability of NSAIDs such as sulindac and celocoxib to not only prevent colorectal neoplasia but also to reverse the process of carcinogenesis is strong [20, 21], the biochemical mechanisms underlying sulindac action are not clear. Our current view of the chemopreventitive action of sulindac is the selective proapoptotic effect and inhibition of angiogenesis; two cellular processes which are effective in suppressing tumor proliferation and malignant transformation [4, 22]. NSAIDs reduce prostaglandin (PG) synthesis by inhibiting the activity of COX, a rate-limiting enzyme for synthesis of eicosanoids (PGs, prostacyclin, and thromboxane A2) from arachidonic acid through the unstable intermediates PGG2 and PGH2. Two isoforms of COX (COX-1 and COX-2) have been identified. Whereas COX-1 is constitutively expressed in most tissues, COX-2 is induced by cytokines, growth factors, and tumor promoters in a variety of situations such as inflammation, ovulation, and cancer. COX-2 appears to play an important role in CRC, being up-regulated in colorectal adenomas and adenocarcinomas when compared with adjacent normal mucosa [23]; interestingly, no change in COX-1 gene expression was observed. These findings have instigated numerous studies aimed at inhibiting COX-2 as a means of CRC prevention. In these studies, signaling pathways involving induction of apoptosis, inhibition of tumor angiogenesis, and inhibition of proliferation have been targeted. An alternative COX-independent mechanism of action of sulindac and its metabolites involves its direct binding to peroxisome proliferator-activated receptors (PPARs), especially the δ- and γ-isoforms. (PPAR is a ligand-activated transcription factor of the nuclear hormone receptor superfamily – *i.e.*, nuclear eicosanoid receptor – with three isoforms, α, γ, and δ, present in humans.) While PPARγ can act as a potential tumor suppressor [24–26], PPARδ is a reported oncogene [27, 28] in CRC. For a recent review of the role of NSAIDs in colon cancer progression and underlying mechanisms of action, see Antonakopoulos and Karamanolis [29]. While most proteomics-based studies on NSAID action in CRC have focused on cellular proteins, no systematic analyses on secreted proteins has been performed to date.

Proteins secreted from cells (the secretome) comprise both soluble-secreted proteins as well as proteins associated with secreted membrane vesicles (*e.g.*, exosomes) – for a recent review see [30]. In the context of the tumor microenvironment, the secretomes of tumor cells and stromal cells (comprising cytokines, chemokines, growth factors, proteases, protease inhibitors, *etc.*) play a seminal role in multidimensional protein–protein interactions that influence the growth rate and metastasis of tumor cells [31–35]. Identifying and characterizing colon tumor cell secretome proteins whose expression levels are modulated by sulindac will improve our understanding of the mechanisms underlying the chemopreventitive action of this NSAID on CRC.

As a first step toward understanding NSAID-mediated anticancer activity in the context of the tumor microenvironment, we have used the human colon carcinoma cell line LIM1215 to monitor the effect of sulindac on secretome protein expression levels. In this study, we have systematically explored and optimized sample processing (*e.g.*, secretome preparation) and analysis methods (*e.g.*, DIGE) to define conditions that enable us to examine the possible role of sulindac in the tumor environment. Such a study provides the foundation for a better understanding of the chemopreventitive effects of sulindac on colon cancer.

2   Materials and methods

2.1   Cell culture and reagents

The human colon carcinoma cell line LIM1215 [36] was routinely cultured on 150-mm diameter cell culture dishes (2×10^6 cells/dish) in RPMI 1640 medium (Invitrogen, Carlsbad, CA) supplemented with 5% FCS (CSL, Melbourne), 100 U penicillin and 100 μg/mL streptomycin (Sigma, St. Louis, MO), at 10% CO_2 atmosphere and 37°C until subconfluent (80–90%). Media, supplemented with sulindac (0.2–1 mM), were prepared by adding appropriate aliquots of a 1 M stock solution of freshly prepared sulindac (Sigma) in 1.5 M Tris-HCl, pH 8.5 to RPMI 1640; for control studies (*i.e.*, no sulindac) an identical volume of 1.5 M Tris-HCl, pH 8.5 buffer solution was added to RPMI 1640 media.

2.2   Cell proliferation and viability assays

Cell proliferation was monitored by reduction of 3-(4,5-dimethylthiazol-2-yl)-2,5-diphenyltetrazolium bromide (MTT) absorbance at 595 nm, which corresponds with living cell number and metabolic activity [37]. For cell viability studies, culture media were harvested and centrifuged at $480 \times g$ to collect nonadherent cells. Adherent cells were trypsinized and harvested by centrifugation at $480 \times g$. Both adherent and nonadherent cells were combined and viability assessed in triplicate by phase-contrast microscopy using Trypan Blue dye exclusion (100 μL of 0.4 w/v % Trypan Blue in PBS mixed with 100 μL cell suspension). Cell morphology was

examined using a Nikon TE 2000E microscope equipped with a DP-70 camera.

2.3 Isolation of soluble-secreted proteins and exosomes from LIM1215 culture medium

For the preparation of soluble-secreted proteins and exosomes, subconfluent LIM1215 cells were washed four times in RPMI medium and cultured in serum-free RPMI 1640 medium, in the presence and absence of 1 mM sulindac, for specified time intervals (4, 8, and 16 h treatment). Following sulindac-induced treatment, the conditioned media (CM) from both the sulindac-induced and control cell cultures were harvested by centrifugation at $480 \times g$ for 5 min to sediment nonadherent cells, and the supernatant centrifuged further at $2000 \times g$ for 10 min to remove cellular debris. Complete EDTA-free Protease inhibitor cocktail tablets (Roche) were dissolved in the resultant supernatant. The supernatant was concentrated to ~1 mL using 5000-M_r cut-off Amicon Ultra-15 centrifugal filter devices (Millipore, Billerica, MA). Exosomes were pelleted from each retentate by centrifugation at $100\,000 \times g$ for 1 h at 4°C, the pellet washed twice in PBS and then solubilized in 2-DE sample buffer (7 M urea, 2 M thiourea, 4% CHAPS, and 20 mM Tris-HCl buffer, pH 8.5). The supernatants (soluble-secreted proteins) from both sulindac treated and untreated samples were stored at −80°C. The concentration of each fraction (exosomes and soluble-secreted) was estimated by densitometry using BenchMark Protein Ladder (Invitrogen) as the standard.

2.4 Protein CyDye™ labeling and multiplexing

Both soluble-secreted and exosomal fractions were minimally labeled with fluorescent cyanine dyes (CyDye) according to the manufacturer's instructions (GE Healthcare, Piscataway, NJ). Briefly, 25 μg of each sample was labeled with 200 pmol of either Cy5 (sulindac-treated) or Cy3 (untreated), while the internal standard (25 μg) was labeled with 200 pmol of Cy2, which was generated by pooling 12.5 μg from both sulindac-treated and untreated samples. To eliminate preferential labeling bias, samples were also reverse labeled with CyDye. Labeling was performed for 30 min on ice in the dark and the labeling reactions were quenched by addition of 10 mM lysine (1 μL for each 200 pmol dye) to each reaction tube for 20 min on ice in the dark. The quenched Cy3, Cy5, and Cy2-labeled samples were combined, after which an equal volume of $2 \times$ sample buffer containing 7 M urea, 2 M thiourea, 20 mM DTT, and 1% IPG buffer, pH 3–10 was added to each combined Cy3/Cy5/Cy2 mixture.

2.5 First dimension IPG-phase IEF

2-DE was performed as described previously [38]. Briefly, 24-cm IPG strips (GE Healthcare), with pH values ranging from

3 to 10, were rehydrated with 450 μL of Destreak™ solution (GE Healthcare) for 16 h at 20°C. Rehydrated IPGs were placed on a Manifold plate and labeled samples applied using the cup-loading method. IEF was performed using a Multiphor apparatus (GE Healthcare) at 300 V (3 h), gradient at 1000 V (6 h), gradient at 8000 V (3 h), and step and hold at 8000 V (6 h). IPG strips were equilibrated for 15 min at 23°C in equilibration buffer (6 M urea, 2% SDS w/v, 30% v/v glycerol, 50 mM Tris-HCl (pH 8.8), 1% w/v DTT, and Bromophenol blue) and subsequently for 15 min in equilibration buffer containing 2.5% w/v iodoacetamide, instead of DTT at room temperature.

2.6 Second dimension SDS-PAGE

Equilibrated IPG strips were transferred onto 8–18% gradient polyacrylamide gels cast in low-fluorescence glass plates using an Ettan-DALT caster (GE Healthcare). Gels were run in an Ettan-DALT II electrophoresis unit (GE Healthcare) at 5 W/gel for 30 min and then at a constant 90 V at 23°C until the dye-front reached the bottom of the gel (16 h). The DIGE gels were scanned using a Typhoon 9410 Imager (GE Healthcare) for excitation and emission (488/520, 532/580, and 633/670 nm for Cy2, Cy3, and Cy5, respectively).

2.7 Preparative 2-DE for MS identification

A preparative 2-DE gel containing 400 μg protein from which spots were excised for protein identification *via* MS, was prepared identically, and subjected to the same IEF and SDS-PAGE conditions as the DIGE analytical gels. The pooled sample mixture comprised of (i) sulindac-induced Cy5-labeled soluble secreted protein mixture (25 μg) and Cy3-labeled exosome (25 μg) samples, (ii) untreated Cy5-labeled soluble secreted protein mixture (25 μg) and Cy3-labeled exosome (25 μg) samples, (iii) and a mixture of unlabeled soluble secreted proteins and exosomes from both sulindac-induced and untreated LIM1215 cells (300 μg). Following 2-DE, the gel was fixed in 40% methanol and 7% acetic acid for 30 min, and stained with SYPRO Ruby protein gel stain (Molecular Probes). For Cy3, Cy5, and SYPRO Ruby images, proteins were scanned using a Typhoon 9410 Imager (GE Healthcare). The gel was incubated with a Coomassie R-250 dye-based reagent, Imperial Protein Stain (Pierce Biotechnology) and subsequently scanned using a Personal densitometer (GE Healthcare). Individual gel spots, which were correlated in both analytical and the preparative samples were excised for MS-based protein identification.

2.8 DIGE imaging and DeCyder™ analysis

For each of the DIGE gels, relative quantification of spot intensities and statistical evaluation were analyzed using DeCyder v5.2 software (GE Healthcare). Gels were run in

duplicate for the 4 and 8-h experiments and in triplicate for the 16-h experiments; reproducibility was also confirmed by reversal of Cy3 and Cy5 dyes. DeCyder analysis was performed using Differential In-gel Analysis (DIA) module software for pair-wise comparisons to the pooled internal standard followed by Biological Variation Analysis (BVA) to determine relative expression ratios (*i.e.*, fold-change) between samples using the internal standard to normalize between gels. DIA quantifies protein volume from fluorescence intensity for Cy2, Cy3, and Cy5 and calculates the ratios Cy3/Cy2 (control subjects/internal standard) and Cy5/Cy2 (sulindac-induced treatment/internal standard). Values were then normalized based on the assumption that the amount of protein *per* image is the same. The log ratios of protein volume were calculated and normalized assuming a Gaussian distribution with the assumption that most proteins should remain unchanged and should center at zero (*i.e.*, ratio of 1.0). This approach takes into account gel-to-gel variability over the entire dataset. For this direct analysis, significance levels were determined based on two SDs of the mean volume ratios (95th percentile confidence). One and a half (1.5)-fold increases/decreases of protein expression were classified as significant.

2.9 Spot excision and in-gel trypsinization

Selected Coomassie-stained protein spots were excised using a scalpel from preparative 2-DE gels, extensively washed in deionized water and subjected to automated in-gel trypsinization using a robotic liquid handling workstation (MassPREP™ Station, Waters-Micromass). Briefly, gel plugs were destained, reduced, alkylated, washed, and then dehydrated in 100% ACN. This was followed by incubation with 6 ng/µL trypsin in 50 mM ammonium bicarbonate (25 µL) for 5 h at 37°C. Peptides were extracted once with 1% formic acid/2% ACN, then twice with 50% ACN. Peptide digests were concentrated by centrifugal lyophilization (Savant, USA) to a volume of ~10 µL for direct injection to nano-LC (nLC) ESI-IT MS/MS (LCQ-Deca, Thermo-Fisher, San Jose, USA).

2.10 nLC-MS/MS analysis

Protein digests (1% aqueous formic acid) were transferred into 100 µL glass autosampler vials for injection. Samples were loaded onto an ESI-IT MS (LCQ-Deca, Thermo-Fisher) which was coupled on-line with an RP-nLC (Model 1100 capillary HPLC, Agilent) using a butyl-silica (C4) 150×0.15 mm² id. RP-capillary column (ProteCol™-C4, 3 µm dp, 300 Å, SGE). The column was developed with a linear 60-min gradient from 0 to 100% B with a flow rate of 0.8 µL/min. Solvent A was 0.1% v/v aqueous formic acid and Solvent B was 0.1% aqueous formic acid/60% v/v ACN. The ESI tune parameters were optimized for the maximum sensitivity to detect peptides using angiotensin-I as the peptide

analyte with the following settings: spray voltage, 1.9 kV, capillary temperature, 175°C; and electron multiplier, 1100 V. The mass spectrometer was operated in data-dependent mode (triple-play) to automatically switch between MS (selecting the most intense precursor ion), Zoom (high-resolution MS of the selected precursor ion mass ±5 amu for automated charge state recognition), and MS/MS acquisition for fragmentation using CID. Where four consecutive precursor ions of the same mass were observed, dynamic exclusion was invoked for a period of 240 s.

2.11 Database Searching and analysis

The program extract-msn (Thermo-Fisher) was used to generate peak lists from the LCQ-Deca raw data. Parameters used were as follows: minimum mass 700; maximum mass 5000; grouping tolerance 1.4 Da; intermediate scans 1; minimum group count 1; 10 peaks minimum and TIC of 100 000. Peak lists for each LC-MS/MS run were merged into a single MGF file for MASCOT™ searches (v2.2.01, Matrix Science, UK) [39]. The embedded (MGF file) charge state parameter was set as 1^+, 2^+, 3^+, and 4^+ instructing the MASCOT search algorithm to consider these potential charge states (MASCOT retains the highest-scoring charge state spectrum and discards the others). A subset of the Ludwig nonredundant protein sequence database (created January 2008; URL: ftp://ftp.ch.embnet.org/pub/databases/nr_prot/) was used for all searches (comprising 459 145 entries of human, mouse, rat, bovine, and other closely related organisms sourced from UniProt, PIR, and Ensembl) [40–42]. Database search parameters were as follows: carbamidomethylation of cysteine as a fixed modification (+57 Da) as well as variable modifications consisting of NH_2-terminal acetylation (+42 Da) and oxidation of methionine (+16 Da), and the allowance for up to two missed tryptic cleavages. The peptide mass tolerance was ±3 Da and fragment ion mass tolerance was ±0.8 Da. ESI_Ion-trap was used as the instrument setting for ion-series reporting.

2.12 Data analysis interpretation and protein inference

An in-house software program (*MSPro*) (Kapp *et al.*, manuscript in preparation) was used for parsing and summarizing the output files from the MASCOT search results. Peptide identifications were deemed significant if the IS (ions score) was ≥HS (the homology score) or the identity score if there was no HS. Protein scores were calculated, using the MASCOT *MudPIT* protein scoring scheme, and false-discovery rate calculations were performed as previously described [42]. Briefly, all inferred proteins with a MASCOT *MudPIT* protein score <55, or inferred on the basis of 2 or less significant peptides, were manually validated in accordance with established rules for peptide fragmentation [43].

2.13 Western blot analysis

Western blotting was performed to analyze total cellular proteins, soluble-secreted proteins, and exosomal proteins from sulindac-induced and noninduced LIM1215 cells. Total cellular proteins were obtained by directly lysing cells with lysis solution (9 M urea, 4% CHAPS). Cellular lysates were subsequently centrifuged at 200 000 × *g* for 20 min to remove insoluble cellular debris. Total cellular lysate, soluble secreted protein and exosome fractions were mixed at 1:1 volume ratio with 2 × SDS-PAGE sample buffer (30% glycerol, 2% SDS, 100 mM DTT, 125 mM Tris-HCl, pH 6.8). Total cellular (20 μg), soluble secreted (10 μg), and exosomal (10 μg) proteins were electrophoresed on precast 4–12% SDS Bis-Tris NuPAGE gels (Invitrogen) using MES running buffer (Invitrogen), electro-transferred to NC membranes (Millipore), and blocked in 5% milk in TPBS buffer (0.05% Tween-20 in PBS) for 1 h. Membranes were probed with rabbit anticleaved caspase-3 antibody (Cell Signaling Technology, Boston, MA) (1:1000), mouse anti-Cab45 antibody (BD Biosciences, Franklin Lakes, NJ) (1:1000), and mouse anti-Mac-2 binding protein antibody (Laboratory Diagnostics, NSW, Australia) (1:250) for 2 h, followed by secondary antibody (HRP conjugated antirabbit or antimouse antibodies (1:5000) from BioRad) for 40 min. Antigen–antibody complexes were detected by ECL (GE Healthcare).
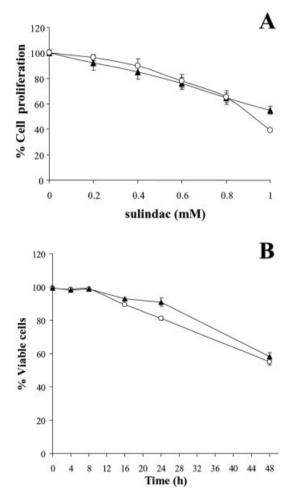
2.14 Protein microarrays

Antibody microarray (Cytokine Human 5.1 kit, RayBiotech, Norcross, GA) experiments were performed on LIM1215 cell secretome, as recommended by the manufacturer. Briefly, cell culture medium (~10 mL) from 1×10^7 cells were concentrated to ~1 mL using a 5000-M_r cut-off Amicon Ultra-15 centrifugal filter device (Millipore). Array membranes were blocked for 1 h and incubated for 16 h at 4°C with 1 mL of concentrated LIM1215 soluble secreted proteins. The array membranes were treated with biotin-conjugated anticytokine antibodies for 2 h. Cytokine detection was achieved with HRP-conjugated streptavidin followed by chemiluminescence and capture of the signals on X-ray films.

3 Results

3.1 Effect of sulindac on cell proliferation and viability

LIM1215 cells were grown in both serum-free media (SFM) and under serum-containing conditions (*i.e.*, 5% FCS) to ensure that the conditioned media (CM) contained minimal exogenous proteins. Seeding density, incubation time in media conditions, volume of media used, type of tissue culture flasks, the effect of differing concentrations of sulindac (0.2–1.0 mM) were all variables that were explored thor-

oughly to select optimal conditions for the rate of proliferation; refer to Section 2 for optimal cell culture conditions selected in this study. Figure 1A demonstrates that sulindac inhibits LIM1215 cell proliferation in the MTT assay in a dose-dependent manner over a concentration range of 0.2–1 mM. Under SFM conditions 50% inhibition of proliferation by 1 mM sulindac treatment was observed. Accordingly, 1 mM sulindac was used in all experiments performed in this study. A comparison of SFM and serum-containing culture conditions over 0.2–1 mM of sulindac demonstrated only a marginal difference in the rate of proliferation (Fig. 1A). To minimize cell death and maximize secretome protein concentration, cell viability levels were also measured over a period of 48 h using Trypan Blue dye exclusion assay

Figure 1. Effect of sulindac on LIM1215 cell proliferation and viability. LIM1215 cells were cultured under the serum-containing (▲) and the serum-free (○) conditions. Cells were treated with different concentrations of sulindac for 24 h and proliferation rates were estimated using the MTT assay. Values are means of three samples from one of the three individual experiments. Bars, ±SD (*N* = 3) (A). LIM1215 cells were cultured in 1 mM sulindac for various times and cell viability was determined by Trypan Blue dye exclusion assay. Values are means of triplicate tests. Bars, ±SD (*N* = 3) (B).

(Fig. 1B). Approximately 95% of cells were viable in 5% FCS for 16 h using 1 mM sulindac, compared to ~85% when cultured in SFM; cell viability was reduced to ~55% after 48 h incubation.

To investigate whether the secretome protein profiles were influenced by the nature of the CM conditions, LIM1215 cells were metabolically labeled with ^{35}S-Met and ^{35}S-Cys [44] and treated with 1 mM sulindac under both SFM and serum-containing culture conditions. CMs were concentrated and subjected to 2-DE analysis. Radioautographs of metabolically labeled proteins secreted in SFM and serum-containing CM were indistinguishable (Supporting Information, Fig. S1), validating the experimental approach. For these reasons, all experiments reported in this study were performed at 4, 8, or 16 h using 1 mM sulindac (concentration at which 50% inhibition was observed) in SFM.

3.2 Sulindac-induced morphological changes and apoptosis onset

LIM1215 cells exhibit an epithelial-like morphology in culture [36, 47]; growing as small pleomorphic cells in an adherent monolayer. Upon addition of 1 mM sulindac, the morphology of LIM1215 cells cultured in either SFM or FCS changed progressively over a 24 h period (Fig. 2A). At 8 h incubation, the level of cell–cell contact decreases regardless of SFM/serum-containing media conditions and by 16 h cells assume an elongated (spindle-like) morphology and are less adherent, becoming even more pronounced after 24 h. We next examined the time of onset of apoptosis, as judged

by the appearance of cleaved-and-activated caspase 3 (Fig. 2B). Cleaved caspase-3 was first detected by Western blot analysis after 16 h sulindac treatment, becoming more prominent after 24 h under both SFM and serum-containing conditions (Fig. 2B). The levels of cleaved caspase-3, estimated by densitometry, were approximately six times higher in cells cultured under SFM conditions when compared to cells cultured under serum-containing conditions. These data are consistent with the cell-viability assay data (Fig. 1B), and indicate that after 4 and 8-h treatment of LIM1215 cells with 1 mM sulindac that the CM was minimally contaminated with intracellular proteins derived from apoptotically lysed cells. For this reason we confined our proteomic studies to 1 mM sulindac treatment to preapoptotic conditions (*i.e.*, comparison of protein profiles after 4 and 8 h sulindac with 16 h sulindac treatments).

3.3 Isolation and characterization of soluble-secreted proteins and exosomes

Figure 3A outlines our purification strategy for the isolation of both soluble-secreted proteins and exosomes from LIM1215 CM. This strategy combines differential centrifugation of the CM to remove cell debris followed by concentration of the CM by centrifugal passage through a 5K NMW cut-off membrane. Exosomes were harvested from the retentate by centrifugation (100 000 × g, 1 h) and washed twice with PBS prior to further study; typically, protein yields for recovered exosomal proteins and soluble-secreted proteins were approximately 20–50 µg and 0.5 mg *per* ~3×10^8
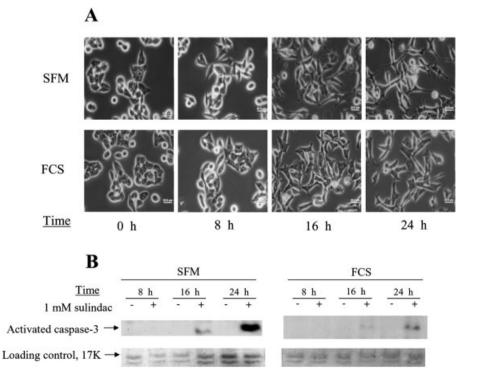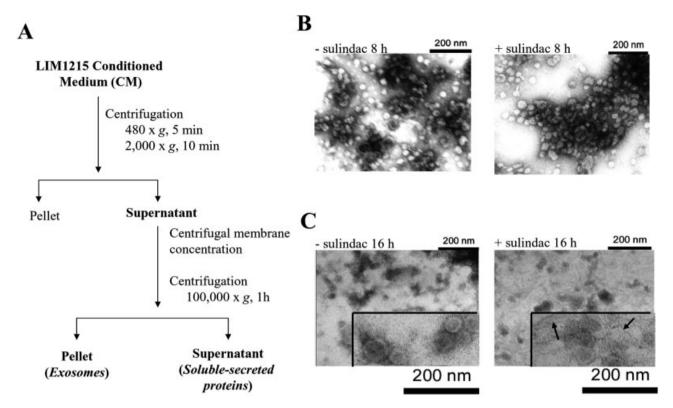

Figure 2. Effect of sulindac on LIM1215 cell morphology and onset of apoptosis. LIM1215 cells were cultured in 1 mM sulindac under serum-free (SFM) and serum-containing (FCS) conditions for various time periods (8–24 h). Cells were digitally photographed using a TE 2000E microscope equipped with a DP-70 camera (A). Total cellular proteins were prepared as described in Section 2, separated by SDS-PAGE and transferred onto an NC membrane. Cleaved and activated caspase-3 was detected by Western blotting using an anticleaved caspase-3 antibody (B). Loading control images were obtained by subsequent staining (deep purple dye) of membranes after Western blotting.

Figure 3. Isolation and characterization of LIM1215 cell secretome. Schema of isolation strategy for soluble-secreted proteins and exosomes from the CM of LIM1215 cells (A). Electron micrographs of purified exosomes (B and C) negatively stained with uranyl acetate and examined at 60 kV. After 8 h sulindac treatment, exosomes are homogeneous, round-shaped membrane vesicles (30–100 nm diameter). After 16 h sulindac treatment EM images also reveal the presence of ellipsoid (cigar-shaped) vesicles (indicated by arrows in the enlarged insert).
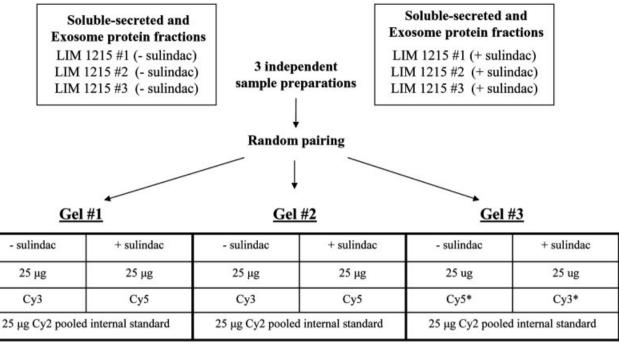
cells (10×150-mm^2 dishes) *per* 8–16 h, respectively. Treatment in the presence and absence of 1 mM sulindac, particularly up to 8 h treatment, did not significantly affect protein yields. To confirm that membranous vesicles recovered were indeed enriched for exosomes, they were examined by electron microscopy (EM) (Figs. 3B and C). The EMs of the exosomes from sulindac-treated and untreated LIM1215 cells after 8 h incubation revealed round-shaped homogenous membrane vesicular structures with a size of approximately 30–100 nm, similar to previously described [46–48]. Western blot analysis revealed the presence of CD9, A33, Tsg101, and hsp70, consistent with previous reports for the molecular composition of exosomes [30] (data not shown). Intriguingly, the EMs from LIM1215 cells treated with sulindac for 16 h incubation revealed the presence of ellipsoid (cigar shaped) membranous vesicles of heterogeneous size (Fig. 3C).

3.4 Comparative proteomic analysis of secretome proteins dysregulated by sulindac treatment

2-D DIGE [49], as previously described [38], in combination with LC-MS/MS, was used to electrophoretically separate and identify soluble-secreted and exosomal proteins whose expression levels were dysregulated as a consequence of sulindac treatment. DIGE involves preseparation fluorescent protein labeling with three separate dyes to reduce gel-to-gel variability, to increase sensitivity and dynamic range of protein detection, and to enhance quantification [50]. For the 4 and 8-h incubation time periods, both exosomes and soluble-secreted proteins were independently extracted from LIM1215 cell CM, in either the presence or absence of 1 mM sulindac by performing two independent sample preparations; in the case of the 16-h time period, samples were prepared in triplicate (Fig. 4). Sulindac-treated and untreated samples were randomly paired for comparison. To minimize false positive results due to preferential labeling of proteins with one or other dye, samples were reverse labeled. The intensity of spots in Cy5 and Cy3 2-D images were normalized to the corresponding Cy2 images. Protein spots shaded red, green, and yellow were indicative of their expression levels being increased, decreased, or remaining the same, respectively, upon treatment with 1 mM sulindac.

Approximately 2000 protein spot-features were visualized in each 2-DE gel (there was considerable overlap in proteins from the soluble-secreted protein and exosome protein fractions; data not shown); the most extensive number of protein spot-features being observed in samples from the

Figure 4. 2-D DIGE experimental design and dye/sample allocation for each gel performed for 16 h sulindac treatment.

16-h time point intervals. The gel with the highest number of spot features was used as the master gel for matching the remaining two gels (in the case of 16-h sulindac treatment); the spot features from sulindac-treated and untreated samples were compared using both DIA and BVA modules of the DeCyder software. While using 2SD as threshold the expression levels for *ca*. 93% of the protein spot features were similar, *ca*. 3.1 and 2.3% were significantly down-regulated in the soluble-secreted and exosome fractions, respectively; *ca*. 4.7 and 4.1% protein spot features were up-regulated in these fractions, respectively. Selected protein spot-features (from soluble-secreted protein and exosome fractions, 150 in total), including those whose expression levels were dysregulated by >1.5 fold (19 soluble-secreted proteins and 22 exosomal proteins; 41 in total) by sulindac treatment were excised from the preparative gel (Supporting Information, Fig. S1) and subsequently identified by LC-MS/MS (Supporting Information, Table S1), as described in Section 2.

3.5 Identification of secretome proteins dysregulated by sulindac treatment

LIM1215 proteins whose expression levels were significantly dysregulated upon 1 mM sulindac treatment over 4, 8, and 16-h time periods, their standardized protein spot ratios, experimental and theoretical pI values, and apparent molecular masses (M_r) are listed in Tables 1 (exosomal proteins)

and 2 (soluble-secreted proteins). A comprehensive list of peptide identifications and inferred proteins is given in Supporting Information, Table S1.

3.5.1 Exosomal proteins

The expression levels of at least 22 exosomal proteins (including isoforms) were altered by >1.5-fold after 1 mM sulindac treatment of LIM1215 cells for 16 h, six of which exhibited a two-fold change after 4 and/or 8 h treatment (Table 1 and Supporting Information, Table S1). For example, the Mac-2 binding protein (Mac-2 BP), which was observed in two forms at M_r-97K (pI 3.8–4.4) and M_r-76K (pI 3.6–4.2) (protein spots 11 and 50, respectively, in Figs. 5 and 6) was clearly down-regulated after 4-h (1.2–1.4-fold), and 8-h sulindac treatment (~2.0-fold, ~1.6-fold, respectively); this down-regulation was even more pronounced (~5.8-fold) after 16 h treatment. Confirmation of this finding was provided by Western blot analysis (Fig. 6A), and by reverse labeling of the Cy dyes (Fig. 5). A similar finding was observed for the programmed cell death 6-interacting protein (M_r ~110K, pI ~6.2), also known as Alix, (Fig. 5). Interestingly, one of the profilin isoforms (M_r ~16K, pI ~9.0) (protein spot 148) and several 14-3-3 isoforms, especially ε (M_r ~25K/pI ~4.1, protein spot 91) and the ζ/δ/ε and β/α isoform mixtures (M_r ~25/pI ~4.2, protein spot 92) (Fig. 5 and Table 1), were significantly up-regulated or down-regulated (ε isoform, M_r ~29/pI 3.9, protein

Table 1. Differentially regulated LIM1215 exosomal proteins upon 1 mM sulindac treatment

Gel spot number[a]	Protein name	Acc. number[b]	Standardized protein spot volume ratios[c]			*t*-Test *p*-value[d] 16 h −S/+S	Experimental[e]		Calculated[f]	
			4 h	8 h	16 h		MW (K)	p*I*	MW (kDa)	p*I*
4	Elongation factor 2	P13639	1.6	1.3	1.7	0.003680	110	6.9	101	6.9
6	PDCD6IP (ALIX)	Q8WUM4	−1.9	−2.3	−4.0	0.000626	110	6.2	96	6.1
8	Endoplasmin	P14625	1.1	−1.2	4.9	0.001136	110	5.1	93	4.8
10	Endoplasmin	P14625	1.3	1.6	1.6	0.001562	120	4.2	107	5.7
11	MAC-2 binding protein	Q08380	−1.4	−2.0	−5.9	0.000098	97	4.5	65	5.1
14	78 kDa glucose-regulated protein	P11021	1.4	1.3	1.9	0.003096	87	4.6	72	5.1
29	Adenylyl cyclase-associated protein 1	Q01518	1.3	−1.1	2.1	0.022070	62	9.0	52	8.1
39	Inosine-5′-monophosphate dehydrogenase 2	P12268	1.5	1.4	1.5	0.001187	62	6.7	56	6.4
43	Protein disulfide isomerase A3	P30101	1.2	1.5	1.6	0.000104	57	5.6	57	6
45	Keratin, type II cytoskeletal 8	P05787	−1.3	1.0	−2.0	0.000291	60	5.3	54	5.5
48	Protein disulfide isomerase	P07237	1.2	1.5	1.8	0.012450	66	4.2	57	4.8
50	MAC-2 binding protein	Q08380	−1.2	−1.6	−5.8	0.000271	76	4.0	65	5.1
52	Keratin, type I cytoskeletal 18	P05783	−1.4	−1.2	−1.7	0.000330	50	5.2	48	5.2
52	IL enhancer-binding factor 2	Q12905	−1.4	−1.2	−1.7	0.000330	50	5.2	48	5.3
55	Elongation factor 1-alpha 1	P68104	1.6	1.5	2.0	0.005344	52	9.7	50	9.1
82	60S acidic ribosomal protein	P05388	−1.1	1.1	1.5	0.000046	37	5.9	34	5.7
85	Tropomyosin alpha 3 chain isoform 2	P06753-2	2.2	2.0	2.4	0.002656	31	4.0	33	4.7
86	Tropomyosin alpha 4 chain	P67936	1.8	1.8	1.9	0.007059	31	3.9	28	4.7
87	14-3-3 protein epsilon	P62258	−1.9	−1.7	−3.0	0.046370	29	3.9	29	4.6
91	14-3-3 protein epsilon	P62258	3.6	2.4	1.7	0.000363	26	4.1	29	4.6
92	14-3-3 protein beta/alpha	P31946	4.9	2.3	3.1	0.000001	26	4.2	28	4.6
92	14-3-3 protein epsilon	P62258	4.9	2.3	3.1	0.000001	26	4.2	29	4.5
92	14-3-3 protein zeta/delta	P63104	4.9	2.3	3.1	0.000001	26	4.2	28	4.5
123	GST-P	P09211	1.2	1.1	1.6	0.006891	25	5.0	23	5.9
148	Profilin I	P07737	2.4	3.3	4.7	0.000106	16	9.0	15	8.5

a) Protein gel spot numbers (refer Supporting Information, Fig. S2 and Table S1).
b) Protein accession numbers were from the Uniprot database, http://www.ebi.uniprot.org/index.shtm.
c) The protein content ratio between sulindac-treated and untreated for each specific protein spot. Ratios were generated using DeCyder software, as detailed in Section 2. The higher ratios (>1) indicate exosomal proteins whose expression levels were up-regulated upon 1 mM sulindac treatment, while lower ratios (<−1) indicate exosomal proteins were down-regulated upon 1 mM sulindac treatment.
d) *t*-Test probability values were generated by analyzing experiments in triplicate using DeCyder software. These values are representative of sulindac treatment (±S) for the 16 h incubation period.
e) The experimental molecular mass (K) and p*I* value for each protein.
f) The calculated molecular mass (kDa) and p*I* value for each protein.

spot 87) upon sulindac treatment in a time-dependent manner. Confirmation of these findings was provided in a separate experiment by reverse labeling of the Cy dyes (Fig. 5).

3.5.2 Soluble-secreted proteins

The expression levels of at least 19 soluble-secreted proteins were altered by >1.5-fold after 1 mM sulindac treatment of LIM1215 cells in a time-dependent manner (Table 2, Figs. 6B and 7). For example, the expression levels of two Ca^{2+}-binding proteins, calumenin and Cab45, were significantly increased, especially after 8 h treatment (protein spots 149

and 150, Fig. 7; Supporting Information, Fig. S2; Table 2, Supporting Information, Table S1). Confirmation of this finding was provided by reverse labeling of the Cy dyes and, in the case of Cab45, by Western blot analysis (Fig. 6B). Interestingly, there was no apparent change in total lysate levels of Cab45, as revealed by Western blot analysis (Fig. 6). In contrast to the modestly elevated levels of the exosomal M_r ~16K, p*I* ~9.0 profilin isoform (Fig. 7), the M_r ~16K/ p*I* ~7.7 isoform (spot 145, Fig. 7) was significantly increased after 8 h sulindac treatment. While alterations in the overall 14-3-3 isoform expression profiles were similar in both the soluble-secreted and exosomal fractions, signifi-

Table 2. Differentially regulated LIM1215 soluble-secreted proteins upon 1 mM sulindac treatment

Gel spot number[a]	Protein name	Acc. number[b]	Standardized protein spot volume ratios[c]			t-Test p-value[d] 16 h −S/+S	Experimental[e]		Calculated[f]	
			4 h	8 h	16 h		MW (K)	p*I*	MW (kDa)	p*I*
10	Endoplasmin	P14625	−1.1	1.3	2.5	0.033440	120	4.2	93	4.8
11	MAC-2 binding protein	Q08380	−1.5	−1.8	−9.9	0.007866	97	4.5	96	6.1
14	78 kDa glucose-regulated protein	P11021	1.1	1.5	5.5	0.024630	87	4.6	72	5.1
28	Pyruvate kinase, M1 isozyme	P14618	1.0	1.0	2.0	0.059650	69	9.1	58	8.0
43	Protein disulfide isomerase A3	P30101	−1.1	1.1	2.0	0.001339	65	5.6	57	6.0
47	Tubulin alpha-1B chain	P68363	1.1	1.2	1.8	0.000377	62	4.8	50	5.0
51	Protein disulfide isomerase A6	Q15084	−1.1	1.2	2.2	0.007184	54	4.8	48	5.0
58	Alpha enolase	P06733	1.2	1.2	1.5	0.002726	55	7.2	47	7.0
72	Actin-like protein 2	P61160	−1.1	1.1	1.7	0.020770	44	6.5	45	6.3
76	Creatine kinase, B chain	P12277	1.2	1.3	1.6	0.010530	42	6.6	43	5.3
80	Annexin A2	P07355	−1.2	−1.4	−2.4	0.294100	38	7.2	39	7.6
91	14-3-3 protein epsilon	P62258	1.4	1.7	3.8	0.005326	26	4.1	29	4.6
92	14-3-3 protein beta/alpha	P31946	1.7	1.6	3.1	0.025310	26	4.2	28	4.8
92	14-3-3 protein beta/alpha	P31946	4.9	2.3	3.1	0.025310	26	4.2	28	4.6
92	14-3-3 protein epsilon	P62258	4.9	2.3	3.1	0.025310	26	4.2	29	4.5
93	Chloride intracellular channel protein 1	O00299	1.0	1.1	2.1	0.004989	30	4.8	27	5.1
138	Ubiquitin-conjugating enzyme E2 N	P61088	−1.3	1.1	1.5	0.020060	17	5.8	17	6.1
144	Beta-2-microglobulin	P61769	1.0	−1.1	−2.7	0.000525	14	6.4	14	6.1
145	Profilin I	P07737	1.2	4.1	2.2	0.001100	15	7.8	15	8.5
149	Calumenin.	O43852	2.6	16.1	4.4	0.014000	45	3.5	37	4.5
150	45 kDa calcium-binding protein	Q9BRK5	7.1	9.9	2.69	0.038000	47	4.1	42	4.8

a) Protein gel spot numbers (refer Supporting Information, Fig. S2 and Table S1).
b) Protein accession numbers were from the Uniprot database, http://www.ebi.uniprot.org/index.shtm.
c) The protein content ratio between sulindac-treated and untreated for each specific protein spot. Ratios were generated using DeCyder software, as detailed in Section 2. The higher ratios (>1) indicate soluble-secreted proteins whose expression levels were up-regulated upon 1 mM sulindac treatment, while lower ratios (<−1) indicate soluble-secreted proteins were down-regulated upon 1 mM sulindac treatment.
d) *t*-Test probability values were generated by analyzing experiments in triplicate using DeCyder software. These values are representative of sulindac treatment (±S) for the 16 h incubation period.
e) The experimental molecular mass (K) and p*I* value for each protein.
f) The calculated molecular mass (kDa) and p*I* value for each protein.

cantly elevated levels of protein spots 91 (ε isoform) and 92 (ζ/δ/ε and β/α isoforms) were observed after 16 h treatment with sulindac (Fig. 7, Table 2). Confirmation of these findings was provided by reverse labeling of the Cy dyes and, in the case of Cab45, by Western blotting (Fig. 6B and Fig. 7).

3.5.3 Cytokine/growth factors

Because the concentration of cytokines and growth factors in biospecimens are typically very low (*e.g.*, ng–pg levels) they are not amenable to most MS-based identification methods – unless an extensive enrichment strategy is invoked. For this reason we employed a limited antibody array procedure. Fifteen cytokines were reliably detected (>40% of the intensity of the positive controls) in LIM1215 cell CM (Fig. 8); the most prominent being growth related

oncogene (GRO) and interleukin 8 (IL-8) and, to a lesser extent, insulin-like growth factor binding protein (IGFBP-1) and tissue inhibitor of metalloproteinases (TIMP2). In most cases, the levels of these cytokines and growth factors decreased in LIM1215 CM upon treatment of the cells with 1 mM sulindac.

4   Discussion

Experiments in rodents, *in vitro* studies in CRC cell lines and epidemiological studies show that NSAIDs have anti-tumorigenic activities against CRC [52–55]. Sulindac, an NSAID, inhibits CRC in animal studies [12, 13] and causes regression of adenomas [20, 29, 55] in patients with familial adenomatous polyposis (FAP) coli. Although much work has
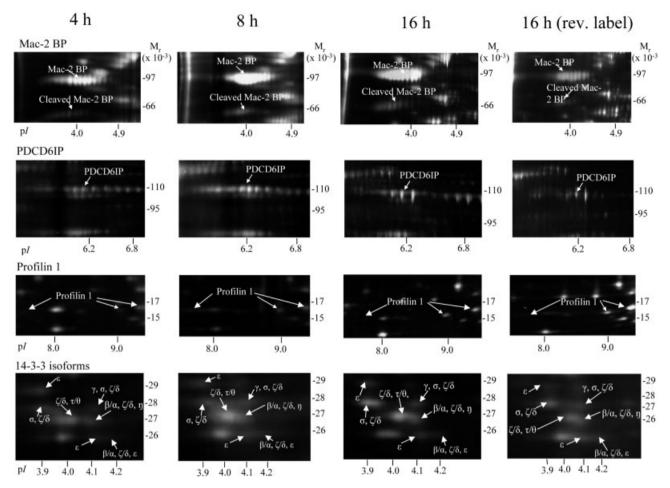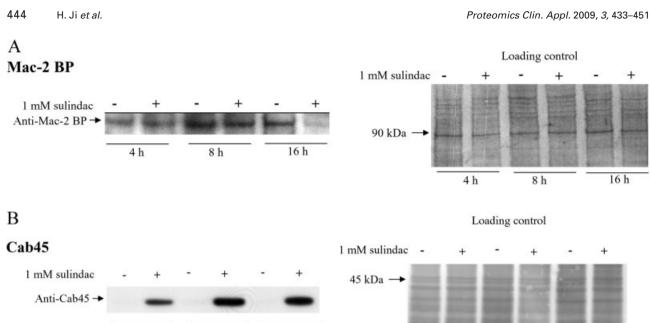
Figure 5. 2-D DIGE analysis of exosomal proteins from sulindac-treated LIM1215 cells. Three Cy-Dye-labeled extracts (25 μg protein each) were combined and separated by 2-DE (see Section 2). Selected exosomal proteins whose protein levels were dysregulated upon 1 mM sulindac treatment are annotated. Reverse-labeled images (*i.e.,* where the Cy3 and Cy5 dyes were reversed in a separate experiment) confirm the presence of these dysregulated proteins. Fold changes of these proteins generated by DeCyder™ software are listed in Table 1. MS-based identifications of these proteins are listed in the Supporting Information, Table S1. A colored version of this figure is shown in Supporting Information Fig. S3, where up-regulated proteins are colored in red, and down-regulated proteins in green.

been performed on the chemopreventitive actions of sulindac and its metabolites, the underlying mechanisms of action are still poorly understood. In this study, we describe, for the first time, a proteomic profiling strategy for analyzing the temporal effect of sulindac treatment over 16 h on the secretome of the LIM1215 CRC cell line. For this study, we devised a facile isolation strategy for fractionating the secretome into its soluble-secreted- and exosomal-protein fractions. This secretome-based strategy is most likely to reveal soluble proteins released from tumor cells into the stroma (tumor microenvironment) at sufficiently high concentrations amenable to current proteome instrumentation [56] and secreted membrane vesicles such as exosomes, which been implicated in cancer cell invasiveness [30]. We found several proteins in the LIM1215 cell secretome, previously not reported, whose expression levels were significantly dysregulated by treatment with 1 mM sulindac prior to onset of

sulindac-induced apoptosis as judged by the appearance of cleaved-and-activated caspase-3.

4.1 Mac-2 binding protein (Mac-2 BP)

Two forms of Mac-2 BP were secreted from LIM1215 cells, the intact molecule ($M_r \sim$ 97K, pI 3.8–4.4) and a cleaved form of lower M_r ($M_r \sim$ 75K, pI 3.6–4.2) [57]; the expression levels of these two forms progressively decreased over 16 h sulindac treatment (Fig. 5) – for example, the levels of Mac-2 BP in both the soluble-secreted and exosomal protein fractions were progressively reduced *ca.* 1.4–1.5-, 1.8–2.0-, and 5.9–10-fold after 4, 8, and 16-h sulindac treatment, respectively (Tables 1 and 2). Mac-2 BP, a secreted glycoprotein of 90–100K, was originally discovered as a tumor-associated antigen 90K in breast cancer [58, 59] and as a ligand that binds galectins (formerly Mac-2)-1, -3, and -7 [57, 60]. It is
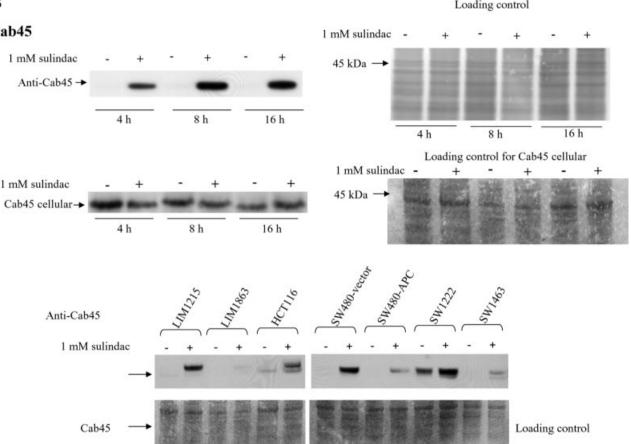
Figure 6. Western blot analyses of Cab45 and Mac-2 binding protein. Exosomes (10 mg) or soluble-secreted proteins (10 mg) isolated from LIM1215 cells treated with 1 mM sulindac (time-course), and selected CRC cell lines, were resolved by SDS-PAGE, blotted onto the NC membranes and probed with Mac-2 BP and Cab45 antibodies as described in Section 2. (A) Exosomal extract from LIM1215 cells probed with Mac-2 BP antibodies; (B) soluble-secreted extract from LIM1215 cells probed with Cab45 antibodies; (C) soluble-secreted extract from selected CRC cell lines probed with Cab45 antibodies. Loading control images were obtained by subsequent staining (deep purple dye) of membranes after Western blotting.

secreted by several different cell types, including hematopoietic cells and glandular or mucosal epithelial cells [57, 60]. A recombinant form of Mac-2 BP has been reported to be susceptible to proteolysis, generating a cleaved form of lower-M_r [57]. Elevated expression levels of Mac-2 BP has been reported to be associated with shorter survival, increased metastasis, and resistance to chemotherapy in

patients with several different types of malignancy, including breast cancer [58], lung cancer [61], colon cancer [62], prostate cancer [63], non-Hodgkin's lymphoma [64], and ovarian cancer. Although the biological functions of Mac-2 BP are poorly defined, it has been implicated in collagen, fibronectin, and β1-integrin binding in the extracellular matrix (ECM) and a possible role in promotion of cell
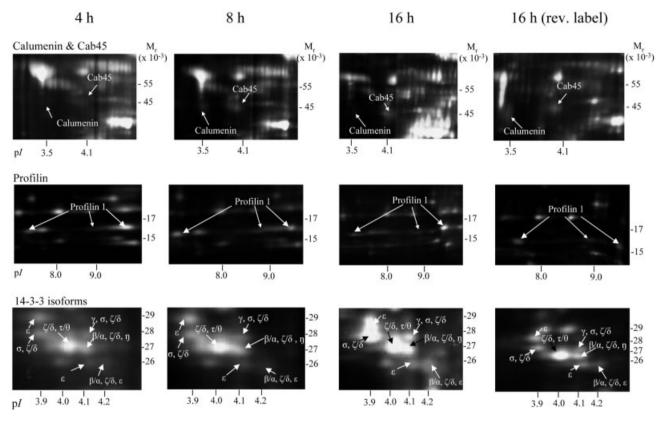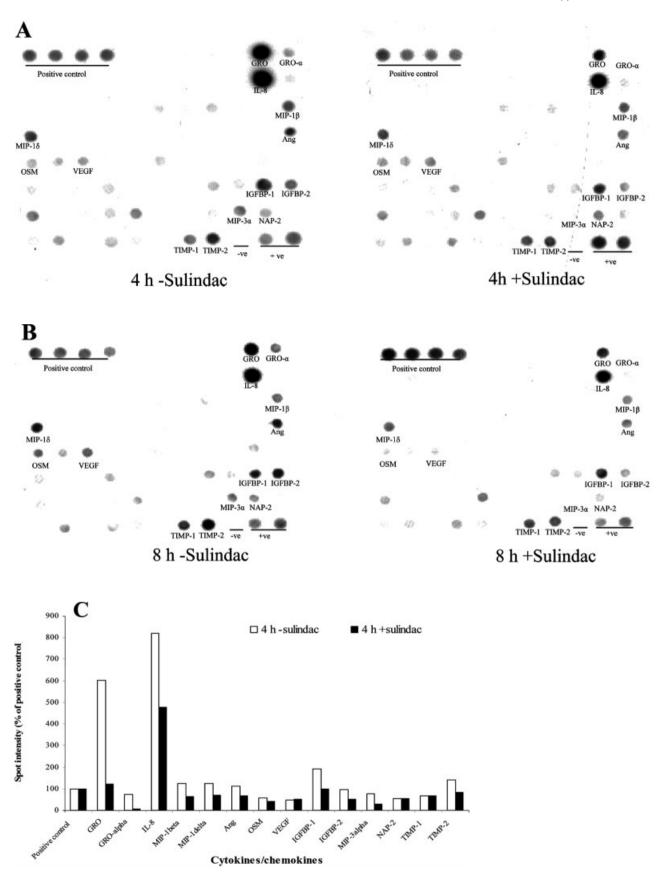
Figure 7. 2-D DIGE analysis of soluble-secreted proteins from sulindac-treated LIM1215 cells. Three CyDye-labeled extracts (25 μg protein each) were combined and separated by 2-DE (see Section 2). Selected soluble-secreted proteins whose protein levels were dysregulated upon 1 mM sulindac treatment are annotated. Reverse-labeled images (*i.e.,* where the Cy3 and Cy5 dyes were reversed in a separate experiment) confirm the presence of these dysregulated proteins. Fold changes of these proteins generated by DeCyder™ software are listed in Table 2. MS-based identifications of these proteins are listed in the Supporting Information, Table S1. A colored version of this Figure is shown in the Supporting Information (Fig. S4), where up-regulated proteins are colored in red, and down-regulated proteins in green.
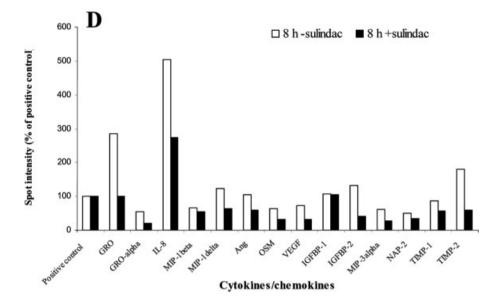
adhesion and invasiveness [65]. Our finding that sulindac significantly reduces the levels of secreted Mac-2 BP prior to the appearance of cleaved-and-activated caspase-3, and *ipso facto* decreases cell adhesion and observed "cell lifting," is consistent with the role of Mac-2 BP in detachment-induced apoptosis, referred to as anoikis [66, 67]. Mac-2 BP is also reported to be a potent immune stimulator [60] inducing production of IL-1 and -6, and other cytokines. Although most of the Mac-2 BP observed in this study was present in the exosomal component of the secretome (nine-fold greater *vs.* soluble-secreted fraction), it is not clear that it is a *bone fida* exosomal protein since ~100 kDa Mac-2 BP monomers have been reported to oligomerize to form ring-shaped 25–45 nm diameter particles [65] that may sediment at the high gravitational force ($100\,000 \times g$) used in this study to isolate exosomes.

4.2 Programmed cell death 6-interacting protein (PDCD6IP)

In this study, the expression levels of exosomal PDCD6IP (also known as apoptosis-linked gene 2 (ALG-2) interacting

protein X (Alix) and AIP-1 [68]), were significantly decreased upon treatment of LIM1215 cells with 1 mM sulindac (Fig. 5, Table 1). Alix is a ubiquitously expressed cytoplasmic protein that localizes to phagosomes and exosomes [30, 68–70]. Alix, and its yeast homolog Bro1, is a class E vacuolar protein sorting (VPS) protein highly conserved in all exosomes characterized to date [30]. Alix/Bro1 interacts with two of the three heteromeric endosomal sorting complex required for transport (ESCRT) protein complexes and Vsp-4, and it has been speculated that Alix may act as a linker between the three ESCRT complexes (for a review, see [71]). In addition to its putative role in exosome biogenesis, Alix has been implicated in apoptosis [72] due to its ability to bind ALG-2, a member of Ca^{2+} binding penta EF-hand protein family to promote apoptosis [68]. Paradoxically, in this study we find that sulindac treatment of LIM1215 cells significantly reduced the expression levels of Alix. Given that the Alix–ALG-2 interaction is calcium-dependent [72], it is reasonable to hypothesize that sulindac may decrease Ca^{2+} levels in the microenvironment by the release of increased levels of calcium-binding proteins such as Cab45 and calumenin (see

A

4 h -Sulindac

4h +Sulindac

B

8 h -Sulindac

8 h +Sulindac

C

Figure 8. Effect of sulindac on secreted cytokine/chemokine levels from LIM1215 cells. Cytokine array membranes were incubated with the CM from sulindac-treated LIM1215 cells, as described in Section 2 (A and B). Arrays were processed according to the manufacturer's instructions and the intensity of the chemiluminescent signal for each spot was quantitated by densitometry. Quantitative differences between cytokine/chemokine secretion levels by sulindac-treatment (4 h (C); 8 h (D)) were evaluated using Image-Quant™ software. Cytokine/chemokine levels are normalized with respect to positive controls on the array membrane.

below). Intriguingly, overexpression of Alix in Hela cells has been shown to promote detachment-induced apoptosis [73, 74].

4.3 Profilin-1

DIGE analysis identified three distinct profilin-1 isoforms with different pI values (spot 145, pI ~7.5; spot 146, pI ~9.0; and spot 148, pI ~10.0), presumably due to varying extents of PTM (Figs. 5 and 7, Tables 1 and 2). Intriguingly, increased expression levels of protein spots 145 and 148 were observed only in the soluble-secreted and exosomal fractions, respectively; expression levels of spot 145 being highest after 8 h sulindac treatment, while maximal expression of spot 148 was observed after 16-h sulindac treatment. The expression levels of the most basic profilin-1 isoform (spot 146), present in both soluble-secreted and exosomal fractions, appeared constant upon treatment of LIM1215 cells with sulindac. Profilins are a class of low-M_r actin-binding proteins that regulate the dynamics of actin polymerization [75, 76]. In addition to interacting with actin, profilin also interacts with several other proteins involved in a diverse range of functions, such as focal adhesion, trafficking, and receptor clustering [77]. In the case of breast cancer cells, decreased expression of profilin-1 has been shown to correlate with tumorigenic phenotypes in breast cancer while its overexpression is reported to suppress tumorigenecity [77]. The nature of cellular compartmentalization of the different isoforms of profilin-1 seen in this study, and the varying PTMs of these isoforms, is not known and must await further experimentation.

4.4 14-3-3 isoforms

In this study, we observed several 14-3-3 isoforms in the LIM1215 secretome that were significantly up- or down-

regulated in a time-dependent manner upon 1 mM sulindac treatment (Fig. 5). For example, in the exosome fraction the expression levels of the ε (M_r ~25K/pI ~4.1, protein spot 91) and β/α and ζ/δ/ε isoforms (M_r ~ 25K/pI ~4.2, protein spot 92) were up-regulated, while the ε isoform (M_r ~29K, pI ~3.9, protein spot 87) was down-regulated. Although alterations in the overall 14-3-3 isoform expression profiles were similar in both the soluble-secreted and exosomal fractions, significantly elevated levels of both ε and β/α/ζ/δ/ε isoforms (M_r ~26K/pI ~4.1–4.2, protein spots 91 and 92) were observed in the exosome fraction after 16-h treatment of the cells with sulindac (Figs. 5 and 7). The increased protein abundances of these 14-3-3 isoforms were also detected in the cellular proteins after sulindac-induced stimulation for the same time periods (Ji *et al.*, unpublished data).

There are seven human 14-3-3 genes encoding the various isoforms of the 14-3-3 protein family [78, 79]. Human 14-3-3 proteins regulate diverse cellular functions that are important in cancer biology such as apoptosis and cell-cycle checkpoints [78]; over 100 cellular protein–protein interactions that involve 14-3-3 have been reported [78–81]. Interestingly, two forms of 14-3-3ε isoform were unambiguously identified by MS as spot features 87 (M_r ~29, pI ~3.9) and 91 (M_r ~26, pI ~4.1) (Table 2); the expression levels for spot features 87 and 91 being down-regulated and up-regulated in LIM1215 cells, respectively, in a time-dependent manner over 16-h treatment. The difference in M_r and pI values for these two forms of 14-3-3ε, presumably, may reflect differences in PTMs or proteolytic cleavage. In the case of the latter, Won *et al.* [80] report lowering (by ~2K) of the M_r of 14-3-3ε by caspase-3 cleavage at Asp238; this, in turn, promotes *Bad*/Bcl-x(L) interactions thereby inducing apoptosis. Our findings are in accord with a recent report by Liou *et al.* [82], which show, by Western blot analysis, that sulindac and other NSAIDs drastically suppress 14-3-3ε and

induce CRC apoptosis *via* the PPARδ/14-3-3ε transcriptional pathway; taken together these data suggest that 14-3-3ε is a potential target for the prevention and therapy of CRC. Interestingly, our findings show that the expression levels of secreted 14-3-3σ appear unchanged over 16 h sulindac treatment; 14-3-3σ has been directly implicated in the etiology of many human cancers and is thought to function as a tumor suppressor by inhibiting cell-cycle progression and by causing cells to leave the stem-cell compartment and undergo differentiation [78].

4.5 Calcium-binding proteins

Our findings show that the expression levels of two secreted proteins, calumenin and Cab45, were significantly elevated upon treatment of LIM1215 cells with 1 mM sulindac. These calcium-binding proteins (albeit low-calcium binding affinity with dissociation constants of ~1 mM) are members of the CREC family of proteins that contain multiple EF-hand domains [83]; CREC is the acronym for four members of this protein family – Cab45, reticulocalbin, ERC-45, and calumenin. Although most of their functions remain unknown, the fact that the CREC family of proteins is highly conserved between species indicates their importance in normal cellular behavior. Cab45 localizes to the Golgi complex [84], while calumenin distributes throughout the entire secretory pathway [85] and is a secreted protein. In our current study, DIGE analysis did not reveal calumenin in the sulindac-untreated LIM1215 secretome, only after 8-h sulindac treatment. Our findings show for the first time that another CREC protein, Cab45, is secreted from LIM1215 cells only after sulindac treatment; western blot analysis revealed a similar phenomenon for several other CRC cell lines such as HCT116, SW480, SW1222, and to a lesser extent, SW1463 (Fig. 6B). It is well recognized that Ca^{2+} plays an important role in cell proliferation [86]. Because internal cellular levels of Ca^{2+} are finite, prolonged bouts of signaling depend on the influx of external Ca^{2+} *via* so-called store-operated Ca^{2+} channels (SOCs) in the plasma membrane. Weiss *et al.* [87] report that the inhibition of SOC entry contributes to the antiproliferative effect of NSAIDs in human CRC cells. It is interesting to speculate that the increased secretion of the Ca^{2+}-binding proteins – Cab45 and calumenin – that we observed may be involved in SOC entry in human CRC cells upon NSAID treatment.

4.6 Growth factors

Protein antibody array was performed to study the effects of sulindac on low abundance cytokine and growth factor secretions. Fifteen cytokines were reliably detected; the most prominent being the tumor growth factors GRO (growth-regulated alpha protein) and IL-8, both members of the CXC subfamily of chemokines [88]. Elevated levels of angiogenic IL-8 have been detected in a variety of cancers [88], including colon carcinoma [89]. GRO-α, originally called "melanoma growths

stimulatory activity", has been shown to function as an autocrine growth factor for melanoma [90], as well as lung and stomach adenocarcinoma cell lines [91]. Both GRO-α and IL-8 exhibit pleiotropism – not only are they autocrine growth factors, but they also display angiogenic activities [88]. The levels of those cytokines/chemokines revealed in our study decreased significantly upon sulindac treatment, which is in agreement with NSAID inhibition of cytokine expression in human monocytes [92] and gastric cancer cells [93].

Establishing the mechanism underlying apoptotic induction by sulindac is an important first step in understanding the potent chemoregressive action of this NSAID in colon adenomas. The results shown in this paper implicate a number of secreted proteins in sulindac action, notably, Mac-2BP, Alix, profilin, 14-3-3-ε and β/α, the CXC chemokines IL-8 and GRO and, especially, the calcium-binding proteins Cab45 and calumenin. The secretome-based proteomics strategy described here, focusing on proteins secreted from tumor cells, provides a tool for identifying potential markers for monitoring the efficacy of chemopreventitive drugs such as sulindac.

5   References

[1] Garcea, G., Sharma, R. A., Dennison, A., Steward, W. P. *et al.*, Molecular biomarkers of colorectal carcinogenesis and their role in surveillance and early intervention. *Eur. J. Cancer* 2003, *39*, 1041–1052.

[2] Selby, J. V., Friedman, G. D., Quesenberry, C. P., Jr., Weiss, N. S., A case-control study of screening sigmoidoscopy and mortality from colorectal cancer. *N. Engl. J. Med.* 1992, *326*, 653–657.

[3] Hawk, E. T., Levin, B., Colorectal cancer prevention. *J. Clin. Oncol.* 2005, *23*, 378–391.

[4] Thun, M. J., Henley, S. J., Patrono, C., Nonsteroidal anti-inflammatory drugs as anticancer agents: Mechanistic, pharmacologic, and clinical issues. *J. Natl. Cancer Inst.* 2002, *94*, 252–266.

[5] Baron, J. A., Cole, B. F., Sandler, R. S., Haile, R. W. *et al.*, A randomized trial of aspirin to prevent colorectal adenomas. *N. Engl. J. Med.* 2003, *348*, 891–899.

[6] Benamouzig, R., Deyra, J., Martin, A., Girard, B. *et al.*, Daily soluble aspirin and prevention of colorectal adenoma recurrence: One-year results of the APACC trial. *Gastroenterology* 2003, *125*, 328–336.

[7] Bertagnolli, M. M., Eagle, C. J., Zauber, A. G., Redston, M. *et al.*, Celecoxib for the prevention of sporadic colorectal adenomas. *N. Engl. J. Med.* 2006, *355*, 873–884.

[8] Beazer-Barclay, Y., Levy, D. B., Moser, A. R., Dove, W. F. *et al.*, Sulindac suppresses tumorigenesis in the Min mouse. *Carcinogenesis* 1996, *17*, 1757–1760.

[9] Moorghen, M., Ince, P., Finney, K. J., Sunter, J. P. *et al.*, A protective effect of sulindac against chemically-induced primary colonic tumours in mice. *J. Pathol.* 1988, *156*, 341–347.

[10] Skinner, S. A., Penney, A. G., O'Brien, P. E., Sulindac inhibits the rate of growth and appearance of colon tumors in the rat. *Arch. Surg.* 1991, *126*, 1094–1096.

[11] Piazza, G. A., Alberts, D. S., Hixson, L. J., Paranka, N. S. *et al.*, Sulindac sulfone inhibits azoxymethane-induced colon carcinogenesis in rats without reducing prostaglandin levels. *Cancer Res.* 1997, *57*, 2909–2915.

[12] Rao, C. V., Rivenson, A., Simi, B., Zang, E. *et al.*, Chemoprevention of colon carcinogenesis by sulindac, a nonsteroidal anti-inflammatory agent. *Cancer Res.* 1995, *55*, 1464–1472.

[13] Boolbol, S. K., Dannenberg, A. J., Chadburn, A., Martucci, C. *et al.*, Cyclooxygenase-2 overexpression and tumor formation are blocked by sulindac in a murine model of familial adenomatous polyposis. *Cancer Res.* 1996, *56*, 2556–2560.

[14] Goldberg, Y., Nassif, I. I., Pittas, A., Tsai, L. L. *et al.*, The antiproliferative effect of sulindac and sulindac sulfide on HT-29 colon cancer cells: Alterations in tumor suppressor and cell cycle-regulatory proteins. *Oncogene* 1996, *12*, 893–901.

[15] Bigler, J., Whitton, J., Lampe, J. W., Fosdick, L. *et al.*, CYP2C9 and UGT1A6 genotypes modulate the protective effect of aspirin on colon adenoma risk. *Cancer Res.* 2001, *61*, 3566–3569.

[16] Ulrich, C. M., Bigler, J., Potter, J. D., Nonsteroidal anti-inflammatory drugs for cancer prevention: Promise, perils and pharmacogenetics. *Nat. Rev. Cancer* 2006, *6*, 130–140.

[17] Martinez, M. E., O'Brien, T. G., Fultz, K. E., Babbar, N. *et al.*, Pronounced reduction in adenoma recurrence associated with aspirin use and a polymorphism in the ornithine decarboxylase gene. *Proc. Natl. Acad. Sci. USA* 2003, *100*, 7859–7864.

[18] Fries, S., Grosser, T., Price, T. S., Lawson, J. A. *et al.*, Marked interindividual variability in the response to selective inhibitors of cyclooxygenase-2. *Gastroenterology* 2006, *130*, 55–64.

[19] Bresalier, R. S., Sandler, R. S., Quan, H., Bolognese, J. A. *et al.*, Cardiovascular events associated with rofecoxib in a colorectal adenoma chemoprevention trial. *N. Engl. J. Med.* 2005, *352*, 1092–1102.

[20] Giardiello, F. M., Hamilton, S. R., Krush, A. J., Piantadosi, S. *et al.*, Treatment of colonic and rectal adenomas with sulindac in familial adenomatous polyposis. *N. Engl. J. Med.* 1993, *328*, 1313–1316.

[21] Steinbach, G., Lynch, P. M., Phillips, R. K., Wallace, M. H. *et al.*, The effect of celecoxib, a cyclooxygenase-2 inhibitor, in familial adenomatous polyposis. *N. Engl. J. Med.* 2000, *342*, 1946–1952.

[22] Gasparini, G., Longo, R., Sarmiento, R., Morabito, A., Inhibitors of cyclo-oxygenase 2: A new class of anticancer agents? *Lancet Oncol.* 2003, *4*, 605–615.

[23] Eberhart, C. E., Coffey, R. J., Radhika, A., Giardiello, F. M. *et al.*, Up-regulation of cyclooxygenase 2 gene expression in human colorectal adenomas and adenocarcinomas. *Gastroenterology* 1994, *107*, 1183–1188.

[24] Sarraf, P., Mueller, E., Jones, D., King, F. J. *et al.*, Differentiation and reversal of malignant changes in colon cancer through PPARgamma. *Nat. Med.* 1998, *4*, 1046–1052.

[25] Kohno, H., Yoshitani, S., Takashima, S., Okumura, A. *et al.*, Troglitazone, a ligand for peroxisome proliferator-activated receptor gamma, inhibits chemically-induced aberrant crypt foci in rats. *Jpn. J. Cancer Res.* 2001, *92*, 396–403.

[26] DuBois, R. N., Gupta, R., Brockman, J., Reddy, B. S. *et al.*, The nuclear eicosanoid receptor, PPARgamma, is aberrantly expressed in colonic cancers. *Carcinogenesis* 1998, *19*, 49–53.

[27] He, T. C., Chan, T. A., Vogelstein, B., Kinzler, K. W., PPARdelta is an APC-regulated target of nonsteroidal anti-inflammatory drugs. *Cell* 1999, *99*, 335–345.

[28] Park, B. H., Vogelstein, B., Kinzler, K. W., Genetic disruption of PPARdelta decreases the tumorigenicity of human colon cancer cells. *Proc. Natl. Acad. Sci. USA* 2001, *98*, 2598–2603.

[29] Antonakopoulos, N., Karamanolis, D. G., The role of NSAIDs in colon cancer prevention. *Hepatogastroenterology* 2007, *54*, 1694–1700.

[30] Simpson, R. J., Jensen, S. S., Lim, J. W. E., Proteomic profiling of exosomes: Current perspectives. *Proteomics* 2008, *8*, 4083–4099.

[31] Joyce, J. A., Therapeutic targeting of the tumor microenvironment. *Cancer Cell* 2005, *7*, 513–520.

[31] Radisky, D. C., Bissell, M. J., Cancer. Respect thy neighbor! *Science* 2004, *303*, 775–777.

[32] Kalluri, R., Zeisberg, M., Fibroblasts in cancer. *Nat. Rev. Cancer* 2006, *6*, 392–401.

[33] Minchinton, A. I., Tannock, I. F., Drug penetration in solid tumours. *Nat. Rev. Cancer* 2006, *6*, 583–592.

[34] Galon, J., Fridman, W. H., Pages, F., The adaptive immunologic microenvironment in colorectal cancer: A novel perspective. *Cancer Res.* 2007, *67*, 1883–1886.

[35] Whitehead, R. H., Macrae, F. A., St John, D. J., Ma, J., A colon cancer cell line (LIM1215) derived from a patient with inherited nonpolyposis colorectal cancer. *J. Natl. Cancer Inst.* 1985, *74*, 759–765.

[36] Mosmann, T., Rapid colorimetric assay for cellular growth and survival: Application to proliferation and cytotoxicity assays. *J. Immunol. Methods* 1983, *65*, 55–63.

[37] Ji, H., Moritz, R. L., Kim, Y. S., Zhu, H. J., Simpson, R. J., Analysis of Ras-induced oncogenic transformation of NIH-3T3 cells using differential-display 2-DE proteomics. *Electrophoresis* 2007, *28*, 1997–2008.

[38] Perkins, D. N., Pappin, D. J., Creasy, D. M., Cottrell, J. S., Probability-based protein identification by searching sequence databases using mass spectrometry data. *Electrophoresis* 1999, *20*, 3551–3567.

[39] Bairoch, A., Apweiler, R., Wu, C. H., Barker, W. C. *et al.*, The Universal Protein Resource (UniProt). *Nucleic Acids Res.* 2005, *33*, D154–D159.

[40] Hubbard, T., Andrews, D., Caccamo, M., Cameron, G. *et al.*, *Ensembl 2005. Nucleic Acids Res.* 2005, *33*, D447–D453.

[41] Moritz, R. L., Clippingdale, A. B., Kapp, E. A., Eddes, J. S. *et al.*, Application of 2-D free-flow electrophoresis/RP-HPLC for proteomic analysis of human plasma depleted of multi high-abundance proteins. *Proteomics* 2005, *5*, 3402–3413.

[42] Greening, D. W., Glenister, K. M., Kapp, E. A., Moritz, R. L. *et al.*, Comparison of human platelet membrane-cytoskeletal

proteins with the plasma proteome: Towards understanding the platelet-plasma nexus. *Proteomics Clin. Appl.* 2008, *2*, 63–77.

[43] Kapp, E. A., Schutz, F., Reid, G. E., Eddes, J. S. *et al.*, Mining a tandem mass spectrometry database to determine the trends and global factors influencing peptide fragmentation. *Anal. Chem.* 2003, *75*, 6251–6264.

[44] Ji, H., Baldwin, G. S., Burgess, A. W., Moritz, R. L. *et al.*, Epidermal growth factor induces serine phosphorylation of stathmin in a human colon carcinoma cell line (LIM1215). *J. Biol. Chem.* 1993, *268*, 13396–13405.

[45] Parker, A. L., Kadakia, S. C., Maccini, D. M., Cassaday, M. A., Angueira, C. E., Disappearance of duodenal polyps in Gardner's syndrome with sulindac therapy. *Am. J. Gastroenterol.* 1993, *88*, 93–94.

[46] Raposo, G., Nijman, H. W., Stoorvogel, W., Liejendekker, R. *et al.*, B lymphocytes secrete antigen-presenting vesicles. *J. Exp. Med.* 1996, *183*, 1161–1172.

[47] Segura, E., Nicco, C., Lombard, B., Veron, P. *et al.*, ICAM-1 on exosomes from mature dendritic cells is critical for efficient naive T-cell priming. *Blood* 2005, *106*, 216–223.

[48] Skokos, D., Le Panse, S., Villa, I., Rousselle, J. C. *et al.*, Mast cell-dependent B and T lymphocyte activation is mediated by the secretion of immunologically active exosomes. *J. Immunol.* 2001, *166*, 868–876.

[49] Unlu, M., Morgan, M. E., Minden, J. S., Difference gel electrophoresis: A single gel method for detecting changes in protein extracts. *Electrophoresis* 1997, *18*, 2071–2077.

[50] Lilley, K. S., Razzaq, A., Dupree, P., Two-dimensional gel electrophoresis: Recent advances in sample preparation, detection and quantitation. *Curr. Opin. Chem. Biol.* 2002, *6*, 46–50.

[51] Patten, E. J., DeLong, M. J., Effects of sulindac, sulindac metabolites, and aspirin on the activity of detoxification enzymes in HT-29 human colon adenocarcinoma cells. *Cancer Lett.* 1999, *147*, 95–100.

[52] Newmark, H. L., Bertagnolli, M. M., Aspirin and colon cancer prevention. *Gastroenterology* 1998, *115*, 1036.

[53] Gupta, R. A., DuBois, R. N., Aspirin, NSAIDS, and colon cancer prevention: Mechanisms? *Gastroenterology* 1998, *114*, 1095–1098.

[54] Taketo, M. M., Cyclooxygenase-2 inhibitors in tumorigenesis (part I). *J. Natl. Cancer Inst.* 1998, *90*, 1529–1536.

[55] Cruz-Correa, M., Hylind, L. M., Romans, K. E., Booker, S. V., Giardiello, F. M., Long-term treatment with sulindac in familial adenomatous polyposis: A prospective cohort study. *Gastroenterology* 2002, *122*, 641–645.

[56] Ahn, S.-M., Simpson, R. J., Body fluid proteomics: Prospects for biomarker discovery. *Proteomics Clin. Appl.* 2007, *1*, 1004–1015.

[57] Koths, K., Taylor, E., Halenbeck, R., Casipit, C., Wang, A., Cloning and characterization of a human Mac-2-binding protein, a new member of the superfamily defined by the macrophage scavenger receptor cysteine-rich domain. *J. Biol. Chem.* 1993, *268*, 14245–14249.

[58] Iacobelli, S., Arno, E., D'Orazio, A., Coletti, G., Detection of antigens recognized by a novel monoclonal antibody in tissue and serum from patients with breast cancer. *Cancer Res.* 1986, *46*, 3005–3010.

[59] Iacobelli, S., Sismondi, P., Giai, M., D'Egidio, M. *et al.*, Prognostic value of a novel circulating serum 90K antigen in breast cancer. *Br. J. Cancer* 1994, *69*, 172–176.

[60] Ullrich, A., Sures, I., D'Egidio, M., Jallal, B. *et al.*, The secreted tumor-associated antigen 90K is a potent immune stimulator. *J. Biol. Chem.* 1994, *269*, 18401–18407.

[61] Marchetti, A., Tinari, N., Buttitta, F., Chella, A. *et al.*, Expression of 90K (Mac-2 BP) correlates with distant metastasis and predicts survival in stage I nonsmall cell lung cancer patients. *Cancer Res.* 2002, *62*, 2535–2539.

[62] Ulmer, T. A., Keeler, V., Loh, L., Chibbar, R. *et al.*, Tumor-associated antigen 90K/Mac-2-binding protein: Possible role in colon cancer. *J. Cell Biochem.* 2006, *98*, 1351–1366.

[63] Bair, E. L., Nagle, R. B., Ulmer, T. A., Laferte, S., Bowden, G. T., 90K/Mac-2 binding protein is expressed in prostate cancer and induces promatrilysin expression. *Prostate* 2006, *66*, 283–293.

[64] Fornarini, B., D'Ambrosio, C., Natoli, C., Tinari, N. *et al.*, Adhesion to 90K (Mac-2 BP) as a mechanism for lymphoma drug resistance in vivo. *Blood* 2000, *96*, 3282–3285.

[65] Sasaki, T., Brakebusch, C., Engel, J., Timpl, R., Mac-2 binding protein is a cell-adhesive protein of the extracellular matrix which self-assembles into ring-like structures and binds beta1 integrins, collagens and fibronectin. *EMBO J.* 1998, *17*, 1606–1613.

[66] Grossmann, J., Molecular mechanisms of "detachment-induced apoptosis–Anoikis". *Apoptosis* 2002, *7*, 247–260.

[67] Valentijn, A. J., Zouq, N., Gilmore, A. P., Anoikis. *Biochem. Soc. Trans.* 2004, *32*, 421–425.

[68] Trioulier, Y., Torch, S., Blot, B., Cristina, N. *et al.*, Alix, a protein regulating endosomal trafficking, is involved in neuronal death. *J. Biol. Chem.* 2004, *279*, 2046–2052.

[69] Thery, C., Boussac, M., Veron, P., Ricciardi-Castagnoli, P. *et al.*, Proteomic analysis of dendritic cell-derived exosomes: A secreted subcellular compartment distinct from apoptotic vesicles. *J. Immunol.* 2001, *166*, 7309–7318.

[70] Garin, J., Diez, R., Kieffer, S., Dermine, J. F. *et al.*, The phagosome proteome: Insight into phagosome functions. *J. Cell Biol.* 2001, *152*, 165–180.

[71] Babst, M., A protein's final ESCRT. *Traffic (Copenhagen, Denmark)* 2005, *6*, 2–9.

[72] Missotten, M., Nichols, A., Rieger, K., Sadoul, R., Alix, a novel mouse protein undergoing calcium-dependent interaction with the apoptosis-linked-gene 2 (ALG-2) protein. *Cell Death Differ.* 1999, *6*, 124–129.

[73] Wu, Y., Pan, S., Luo, W., Lin, S. H., Kuang, J., Hp95 promotes anoikis and inhibits tumorigenicity of HeLa cells. *Oncogene* 2002, *21*, 6801–6808.

[74] Wu, Y., Pan, S., Che, S., He, G. *et al.*, Overexpression of Hp95 induces G1 phase arrest in confluent HeLa cells. *Differentiation* 2001, *67*, 139–153.

[75] Feldner, J. C., Brandt, B. H., Cancer cell motility – On the road from c-erbB-2 receptor steered signaling to actin reorganization. *Exp. Cell Res.* 2002, *272*, 93–108.

[76] Witke, W., The role of profilin complexes in cell motility and other cellular processes. *Trends Cell Biol.* 2004, *14*, 461–469.

[77] Janke, J., Schluter, K., Jandrig, B., Theile, M. *et al.*, Suppression of tumorigenicity in breast cancer cells by the microfilament protein profilin 1. *J. Exp. Med.* 2000, *191*, 1675–1686.

[78] Hermeking, H., The 14-3-3 cancer connection. *Nat. Rev. Cancer* 2003, *3*, 931–943.

[79] Rosenquist, M., 14-3-3 proteins in apoptosis. *Braz. J. Med. Biol. Res.* 2003, *36*, 403–408.

[80] Won, J., Kim, D. Y., La, M., Kim, D. *et al.*, Cleavage of 14-3-3 protein by caspase-3 facilitates bad interaction with Bcl-x(L) during apoptosis. *J. Biol. Chem.* 2003, *278*, 19347–19351.

[81] Nufer, O., Hauri, H. P., ER export: Call 14-3-3. *Curr. Biol.* 2003, *13*, R391–R393.

[82] Liou, J. Y., Ghelani, D., Yeh, S., Wu, K. K., Nonsteroidal anti-inflammatory drugs induce colorectal cancer cell apoptosis by suppressing 14-3-3epsilon. *Cancer Res.* 2007, *67*, 3185–3191.

[83] Honore, B., Vorum, H., The CREC family, a novel family of multiple EF-hand, low-affinity Ca(2+)-binding proteins localised to the secretory pathway of mammalian cells. *FEBS Lett.* 2000, *466*, 11–18.

[84] Scherer, P. E., Lederkremer, G. Z., Williams, S., Fogliano, M. *et al.*, Cab45, a novel (Ca2+)-binding protein localized to the Golgi lumen. *J. Cell Biol.* 1996, *133*, 257–268.

[85] Vorum, H., Hager, H., Christensen, B. M., Nielsen, S., Honore, B., Human calumenin localizes to the secretory pathway and is secreted to the medium. *Exp. Cell Res.* 1999, *248*, 473–481.

[86] Berridge, M. J., Bootman, M. D., Lipp, P., Calcium – A life and death signal. *Nature* 1998, *395*, 645–648.

[87] Weiss, H., Amberger, A., Widschwendter, M., Margreiter, R. *et al.*, Inhibition of store-operated calcium entry contributes to the anti-proliferative effect of nonsteroidal anti-inflammatory drugs in human colon cancer cells. *Int. J. Cancer* 2001, *92*, 877–882.

[88] Frederick, M. J., Clayman, G. L., Chemokines in cancer. *Expert Rev. Mol. Med.* 2001, *2001*, 1–18.

[89] Brew, R., Southern, S. A., Flanagan, B. F., McDicken, I. W., Christmas, S. E., Detection of interleukin-8 mRNA and protein in human colorectal carcinoma cells. *Eur. J. Cancer* 1996, *32A*, 2142–2147.

[90] Richmond, A., Balentien, E., Thomas, H. G., Flaggs, G. *et al.*, Molecular characterization and chromosomal mapping of melanoma growth stimulatory activity, a growth factor structurally related to beta-thromboglobulin. *EMBO J.* 1988, *7*, 2025–2033.

[91] Fujisawa, N., Sakao, Y., Hayashi, S., Hadden, W. A., III *et al.*, alpha-Chemokine growth factors for adenocarcinomas: A synthetic peptide inhibitor for alpha-chemokines inhibits the growth of adenocarcinoma cell lines. *J. Cancer Res. Clin. Oncol.* 2000, *126*, 19–26.

[92] Housby, J. N., Cahill, C. M., Chu, B., Prevelige, R. *et al.*, Nonsteroidal anti-inflammatory drugs inhibit the expression of cytokines and induce HSP70 in human monocytes. *Cytokine* 1999, *11*, 347–358.

[93] Takehara, H., Iwamoto, J., Mizokami, Y., Takahashi, K. *et al.*, Involvement of cyclooxygenase-2 – Prostaglandin E2 pathway in interleukin-8 production in gastric cancer cells. *Dig. Dis. Sci.* 2006, *51*, 2188–2197.